

Alpha particles in inhomogeneous electrostatic fluctuations

G.J.J. Botha¹, R.J. Hastie², M.G. Haines²

¹ *Department of Applied Mathematics, University of Leeds, Leeds LS2 9JT, UK*

² *Blackett Laboratory, Imperial College, Prince Consort Road, London SW7 2BZ, UK*

In a tokamak plasma large electrostatic fluctuations have been measured near the plasma edge [1] and reduced fluctuations at internal transport barriers in the plasma body [2]. We consider an electrostatic plasma with different amplitude fluctuations in separate regions of its domain. On this background we place charged particles. We hope to shed some light on the behaviour of alpha particles in fusion plasmas [3].

The numerical domain is a Cartesian plane perpendicular to a uniform magnetic field. The Charney-Hasegawa-Mima (CHM) equation [4] evolves an electrostatic potential in this plane. A fixed density gradient in the x direction gives the characteristic length L_n^{-1} in Figure 1(b), which causes a maximum drift velocity $v_* = (cT_e/eB)L_n^{-1}$ to form at the centre of the x axis, flowing in the y direction. The L_n^{-1} drives large amplitude fluctuations of ϕ at the centre of the x axis. The x boundary conditions are $v_* = \phi = 0$, while the y boundary is periodic. The CHM equation is solved spectrally in the y direction, and both the x direction and nonlinear term are finite differenced [5]. By seeding the box with 7 and 11 wavelengths along y , the CHM equation produces the fluctuations in Figure 1(a). This is taken as the initial background state for this study. The initial state can be used as a frozen background on which particles move, or it can be evolved in time using the linear as well as the nonlinear CHM equation.

On this background 4000 test particles are placed, each with the charge-mass ratio of alpha particles. The test particles sample the background field, with no back reaction on the electrostatic field. The particles are not aware of each other. Instead of the usual guiding centre approach [6], the full Lorentz equation is solved using the Boris particle integrator method [7]. The initial positions and distribution of particles are given in Figure 2. The particles are initialized with the velocity $\mathbf{v}_0 = \mathbf{v}_\perp + (\mathbf{E} \times \mathbf{B})/B^2$, which are the gyro-velocity of each particle around its guiding centre, and the local $\mathbf{E} \times \mathbf{B}$ velocity. After initialization the Larmor radii (ρ_α) are free to change in response to the local forces acting on the particles. The diffusion coefficient can be written in terms of

the variance σ , namely $D(t) = \sigma^2(t)/2t$, when a normal distribution is substituted into the diffusion equation. By sampling the instantaneous distribution of the particles, we can quantify particle diffusion in the x direction.

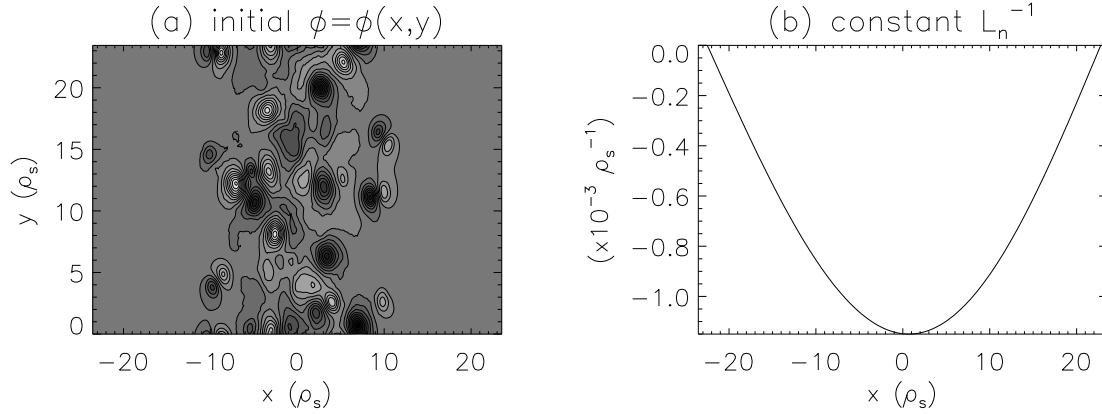


Figure 1: The initial background electrostatic field ϕ (a), and the non-evolving $L_n^{-1} = (1/n_0)dn_0/dx$ profile (b), where $\rho_s = (\text{sound speed})/(\text{ion cyclotron frequency})$.

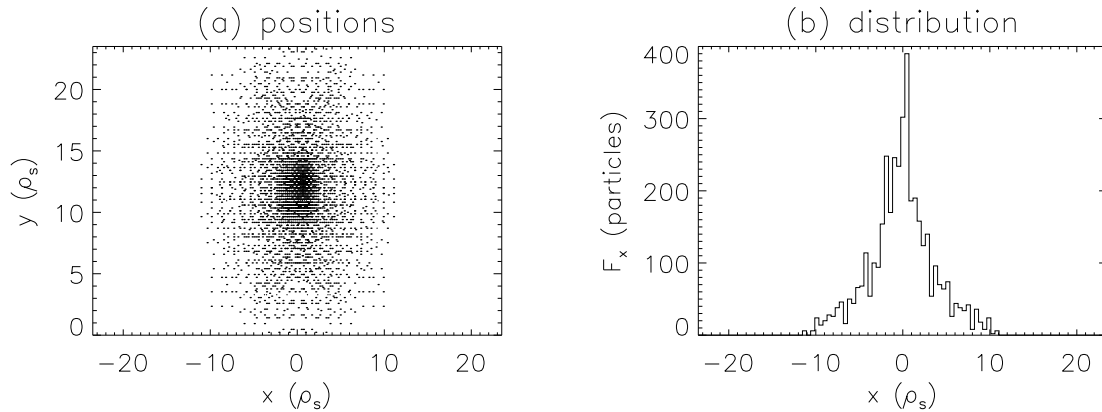


Figure 2: Initial (a) positions and (b) x distribution of particles.

Figure 3 gives the time evolution of the variance for a frozen background field. For initial Larmor radii $\rho_\alpha \leq 1.5\rho_s$ and $\rho_\alpha \geq 3\rho_s$, two rates of change in the variance are observed. The first (faster) rate occurs when all particles sample large $\nabla\phi$ at the centre of the x axis, while the slower rate, measured later during the numerical runs, occurs when a significant fraction of the particles have reached the quiet regions near the x boundaries where $\nabla\phi$ is small. When the variance is not normalized, measurements show that particles initialized with the largest ρ_α spread most into the quiet regions. This is

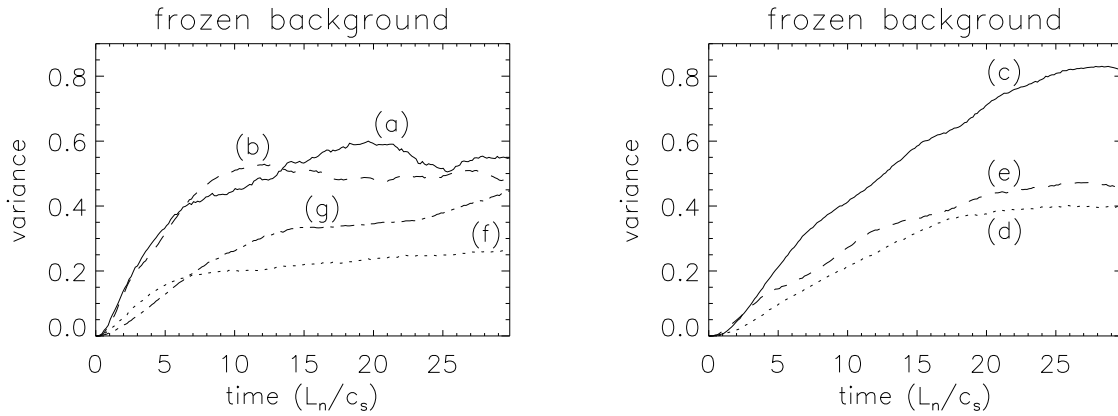


Figure 3: The normalized variance $[\sigma^2(t) - \sigma^2(0)]/\sigma^2(0)$ as a function of time for different ρ_α initializations against a frozen electrostatic background field. The different initializations are labeled as follows: (a) $\rho_\alpha = 0$, (b) $\rho_\alpha = \rho_s$, (c) $\rho_\alpha = 1.5\rho_s$, (d) $\rho_\alpha = 2\rho_s$, (e) $\rho_\alpha = 2.5\rho_s$, (f) $\rho_\alpha = 3\rho_s$, (g) $\rho_\alpha = 4\rho_s$.

because particles are pushed along the x direction while they sample large electrostatic fluctuations at the centre of the x axis. The larger ρ_α , the further they move into the quiet regions while sampling large $\nabla\phi$. The numerical run with initial ρ_α equal to the background vortex radii (Figure 3 curve (c)), shows that although particles are captured by vortices [8], eventually most of them escape and diffuse into the quiet regions.

By considering the change in variance when all particles still sample large $\nabla\phi$ (near the start of runs), we can compare our results directly with those of Manfredi and Dendy [9], who used the guiding centre particle approach in homogeneous background turbulence. Figure 4 shows that when ρ_α is less than the vortex radii of the background, diffusion rates are inhibited by an increase in the finite Larmor radii of the particles [9]. The frozen background has the lowest diffusion rates, while the nonlinear time-evolving background has the highest diffusion rates. Finite Larmor radii allow particles to jump the contour lines of the background field, and when the background field evolve with time (linearly and nonlinearly) the changing potential assists in this process. All runs have the lowest change in their variance when ρ_α is approximately the same size as the radii of the vortices in the background field. When ρ_α increases further, the particles move faster around their guiding centres (as the cyclotron frequency is a constant) and the effective local electric field sampled by the particles is reduced.

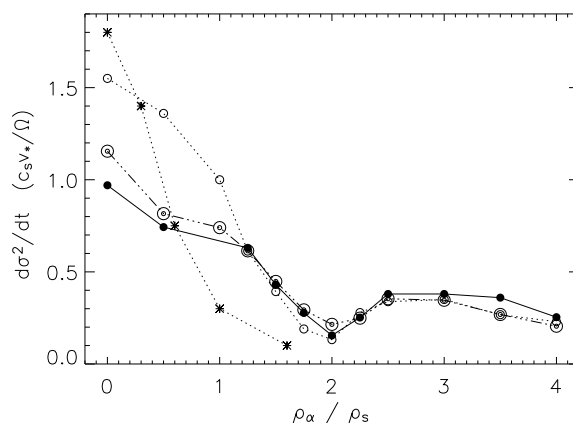


Figure 4: Gradient of σ^2 at $t = 2L_n.c_s^{-1}$. Solid line with solid circles: results with frozen background; dot-dashed line with double circles: results with linear time-evolving background; dotted line with open circles: results with nonlinear time-evolving background. The Manfredi-Dendy [9] result (multiplied by 0.1) is dotted line with stars.

The linear and nonlinear time-evolving electrostatic background fields give similar results to those of the frozen background field (Figure 3). By employing the full Lorentz force on the particles, we have obtained the finite Larmor radius results in the literature, where the guiding centre approximation for the particles was used. We have also extended the diffusion study to cases where the finite Larmor radii are equal to, and larger than the vortex radii in the background field.

- [1] Stangeby P C 2000 *The Plasma Boundary of Magnetic Fusion Devices* (IOP Publishing, Bristol) p 368–77
- [2] Wakatani M, Mukhovatov V S, et al. 1999 *Nuclear Fusion* **39**(12) 2175–249
- [3] Hawryluk R J 1998 *Reviews of Modern Physics* **70**(2) 537–87
- [4] Charney J G 1948 *Geofys. Publ. Kosjones Norsk Videnskap. Akad. Oslo* **17**(2) 1–17
- Hasegawa A & Mima K 1977 *PRL* **39**(4) 205–8
- [5] Botha G J J, Haines M G & Hastie R J 1999 *Phys. Plasmas* **6**(10) 3838–52
- [6] Lee W W 1987 *J. Comp. Physics* **72** 243–69
- [7] Birdsall C K and Langdon A B 1991 *Plasma Physics via Computer Simulation* (IOP Publishing, Bristol) p 55–63
- [8] Annibaldi S V, Manfredi G and Dendy R O 2002 *Phys. Plasmas* **9**(3) 791–9
- [9] Manfredi G and Dendy R O 1996 *PRL* **76**(23) 4360–3